

Analytic properties of the S-matrix and pole trajectories in a separable coupled-channel system

Denny Lane B. Sombillo

RCNP Osaka University

University of the Philippines Diliman

The 1st CENuM Workshop for Hadronic Physics

17-18 June 2019



Outline

- Motivation
- General properties of S-matrix
- Coupled-channel with separable matrix potential
 - S-matrix in single-channel case (uncoupled)
 - S-matrix in coupled-channel case
 - Resonance
 - Resonance-like (rounded cusp) structure
- Distinguishing resonance vs resonance-like structure
- Summary

Motivation

Why coupled-channel system?

The case of $\Lambda(1405)$

- Coupling of the $\pi\Sigma$ and $\bar{K}N$ channels
- Quasi-bound state of $\bar{K}N$
- Appears just below the $\bar{K}N$ threshold

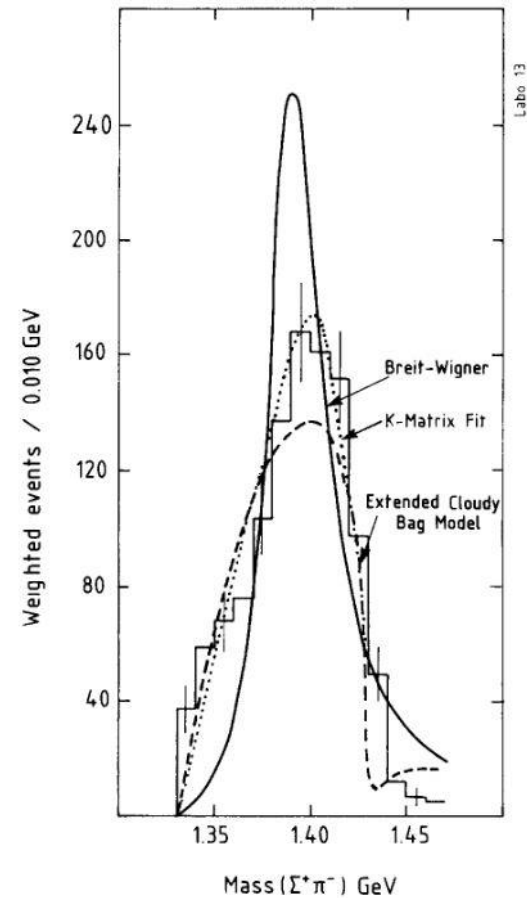
Why S-matrix in complex energy plane?

- Contains information on scattering amplitude.
- Coupled two-channel S-matrix is a function of two-momenta
- Resonance:
 - the peak location \rightarrow real part
 - width \rightarrow imaginary part

Goal: Obtain the general features of scattering observables arising from the coupled-channel system.

R.J. Hemingway, Nuclear Physics B 23 (1973)

R.H. Dalitz and S.F. Tuan, Physical Review Letters 2 (1959)



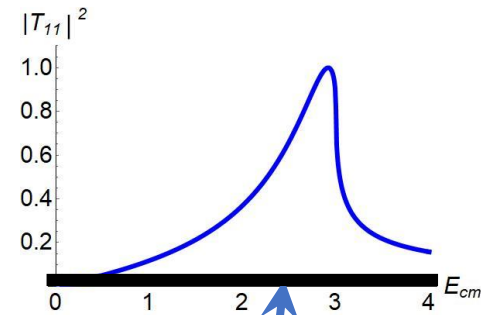
Analytic Properties of S-matrix

The S-matrix (single-channel)

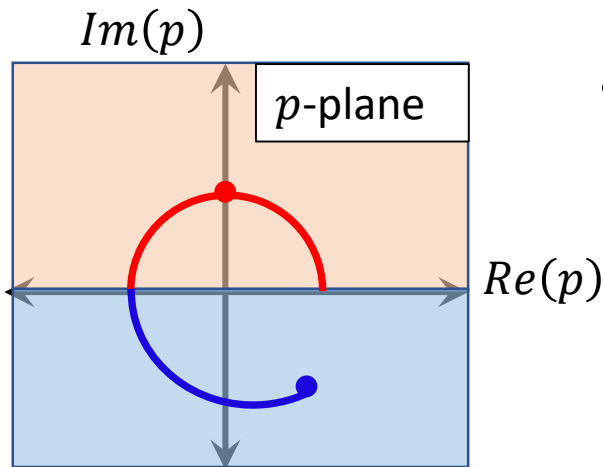
- a single-valued function of the complex momentum p .
- a function of complex E in a two-sheeted Riemann surface

$$E = \frac{p^2}{2\mu}; \quad E = |E|e^{i\theta_E} \quad 0 \leq \theta_E < 4\pi$$

- The physical sheet: $0 \leq \theta_E < 2\pi \rightarrow (Im p > 0)$
- physical region $E = E_R + i0^+ \quad (E_R > 0)$
- The unphysical sheet: $2\pi \leq \theta_E < 4\pi \rightarrow (Im p < 0)$



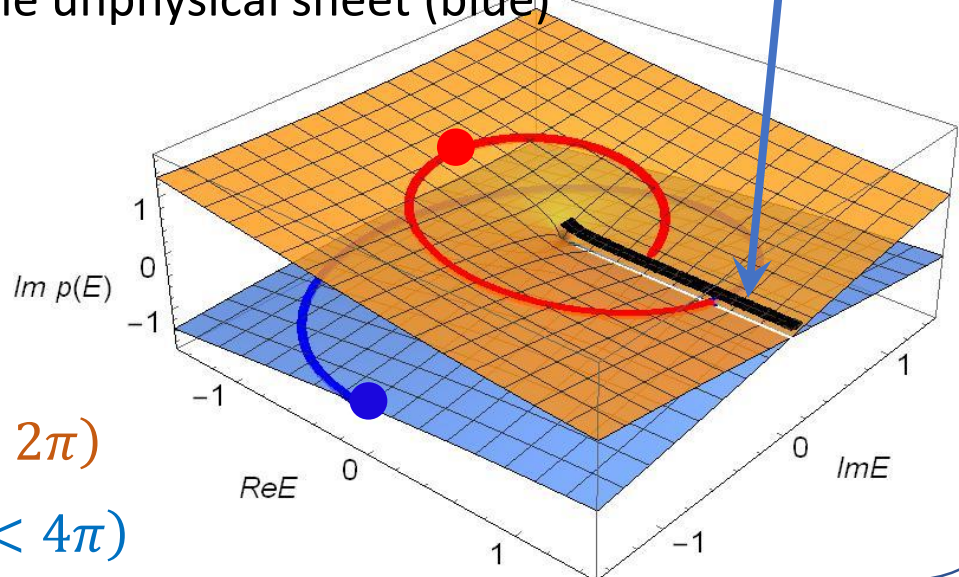
physical region



imaginary part of p in the physical sheet (orange) and in the unphysical sheet (blue)

$$p = \sqrt{2\mu|E|}e^{i\theta_E/2} \quad (0 \leq \theta_E < 2\pi)$$

$$p = \sqrt{2\mu|E|}e^{i\theta_E/2} \quad (2\pi \leq \theta_E < 4\pi)$$



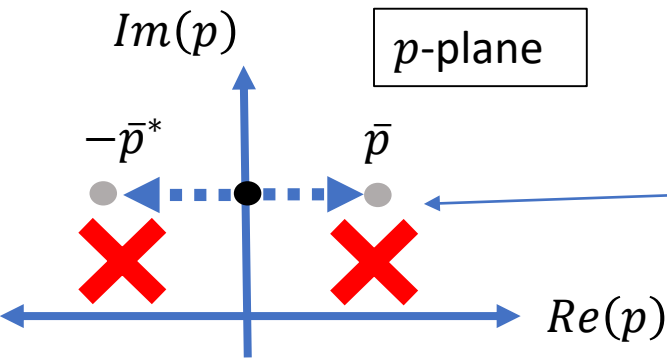
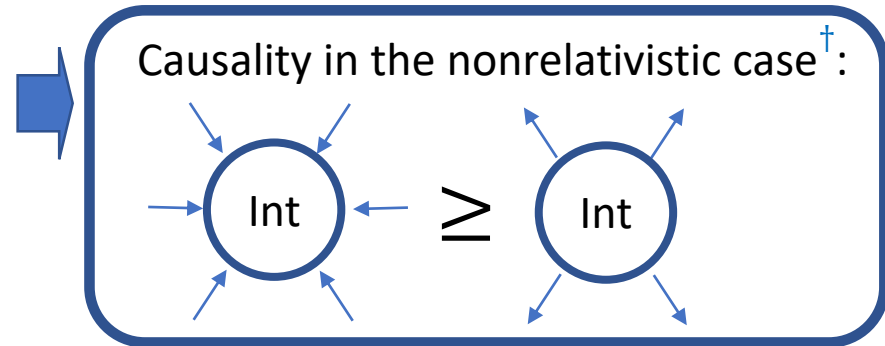
Analytic Properties of S-matrix

Reflection Principle: $S(E) = [S(E^*)]^\dagger$ or $S(p) = [S(-p^*)]^\dagger$

- If E_{pole} is a pole then E_{pole}^* is also a pole.
- The $|S(E_{low})|$ in the lower half E-plane is just a reflection about the real axis of $|S(E_{up})|$ in the upper half.

Poles in the physical sheet

1. Poles in the negative real energy axis are bound states.
2. Poles can only be in the negative real axis.



Results into an exponentially increasing time-dependent wave-function.

No restriction when it comes to poles in the unphysical sheet $Im(p) < 0$.

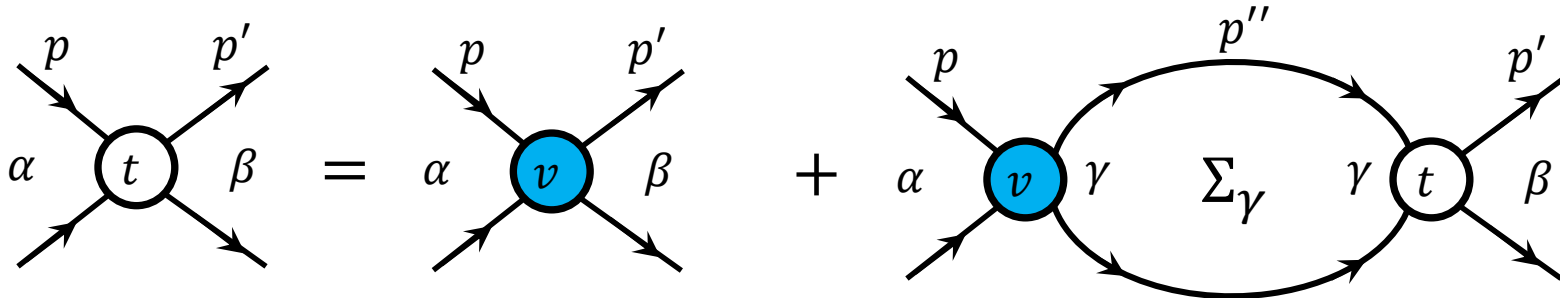
For a single-channel case, the resonance poles are confined only in one unphysical sheet.

† N. G. van Kampen, Phys. Rev. 91 (1953)

Multichannel T-matrix

Lippmann-Schwinger equation:

$$t_{\alpha\beta}(p, p'; E) = v_{\alpha\beta}(p, p') + \sum_{\gamma} \int_0^{\infty} dp'' (p'')^2 \frac{2\mu_{\gamma} v_{\alpha\gamma}(p, p'') t_{\gamma\beta}(p'', p'; E)}{2\mu_{\gamma}(E - \Theta_{\gamma} + i\epsilon) - (p'')^2}$$



$$v_{\alpha\beta}(p, p') = f_{\alpha}(p) \lambda_{\alpha\beta} f_{\beta}(p'); \quad f_{\alpha}(p) = \frac{\beta_{\alpha}^2}{p^2 + \beta_{\alpha}^2} \quad (\text{Yamaguchi form factor})$$

$\lambda_{\alpha\beta}$ is the coupling strength and β_{α} as cut-off parameter

$$t_{\alpha\beta}(p, p'; E) = f_{\alpha}(p) \frac{\text{cof}[\tau(E)^{-1}]_{\alpha\beta}}{\det[\tau(E)^{-1}]} f_{\beta}(p'); \quad [\tau(E)^{-1}]_{\alpha\beta} = (\lambda^{-1})_{\alpha\beta} - \delta_{\alpha\beta} \Sigma(E)_{\alpha};$$

$$\Sigma(E)_{\gamma} = \int_0^{\infty} dp \frac{2\mu_{\gamma} p^2 f_{\gamma}^2(p)}{2\mu_{\gamma}(E - \Theta_{\gamma} + i\epsilon) - (p)^2}$$

Pole position condition:

$$\det[\tau(E)^{-1}] = 0$$

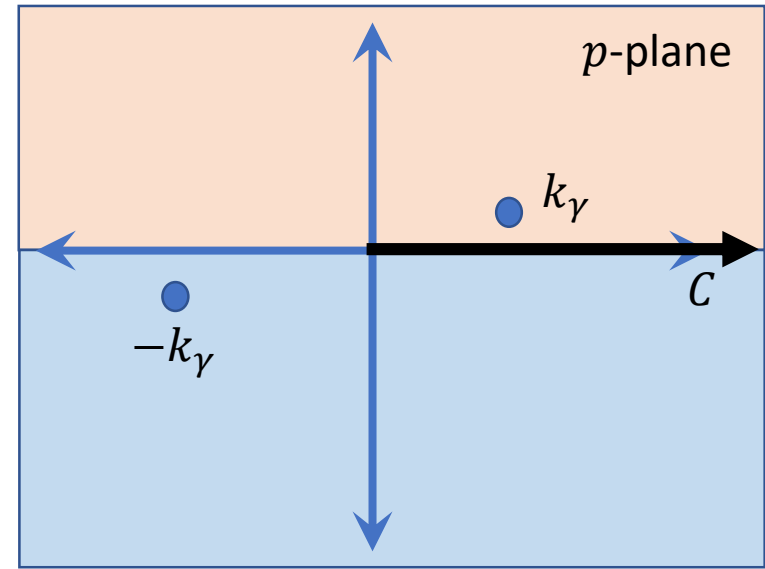
Multichannel T-matrix

$$\Sigma(E)_\gamma = \int_0^\infty dp \frac{2\mu_\gamma p^2 f_\gamma^2(p)}{2\mu_\gamma(E - \Theta_\gamma + i\epsilon) - (p)^2}$$

$$k_\gamma = \pm \sqrt{2\mu_\gamma(E - \Theta_\gamma)}$$

For $f_\gamma(p) = \frac{\beta_\gamma^2}{p^2 + \beta_\gamma^2}$

$$\Sigma(E)_\gamma = \frac{\pi\mu_\gamma\beta_\gamma^3}{2(k_\gamma + i\beta_\gamma)^2}$$



$\Sigma(E)_\gamma$ for E in the physical sheet $k_\gamma = +\sqrt{2\mu_\gamma(E - \Theta_\gamma)}$

$\Sigma(E)_\gamma$ for E in the unphysical sheet $k_\gamma = -\sqrt{2\mu_\gamma(E - \Theta_\gamma)}$

$$S(E) = 1 + 2iT(E); \quad T_{11}(E) = -\pi\mu_1 k_1 f_1(k_1)^2 \text{cof}[\tau(k_1)^{-1}]_{11} / \det[\tau(k_1)^{-1}]$$

$$T_{11}(E) = -\pi\mu_1 k_1 \frac{\beta_1^4}{(k_1^2 + \beta_1^2)^2} \frac{(\lambda^{-1})_{22} - \Sigma(k_2)}{((\lambda^{-1})_{11} - \Sigma(k_1))((\lambda^{-1})_{22} - \Sigma(k_2)) - (\lambda^{-1})_{12}(\lambda^{-1})_{21}}$$

$$(\lambda^{-1})_{\alpha\beta} = \frac{\lambda_{\alpha\beta}}{\lambda_{11}\lambda_{22} - \lambda_{12}\lambda_{21}}$$

Pole-position condition for two-channel case:

$$((\lambda^{-1})_{11} - \Sigma(k_1))((\lambda^{-1})_{22} - \Sigma(k_2)) - (\lambda^{-1})_{12}(\lambda^{-1})_{21} = 0$$

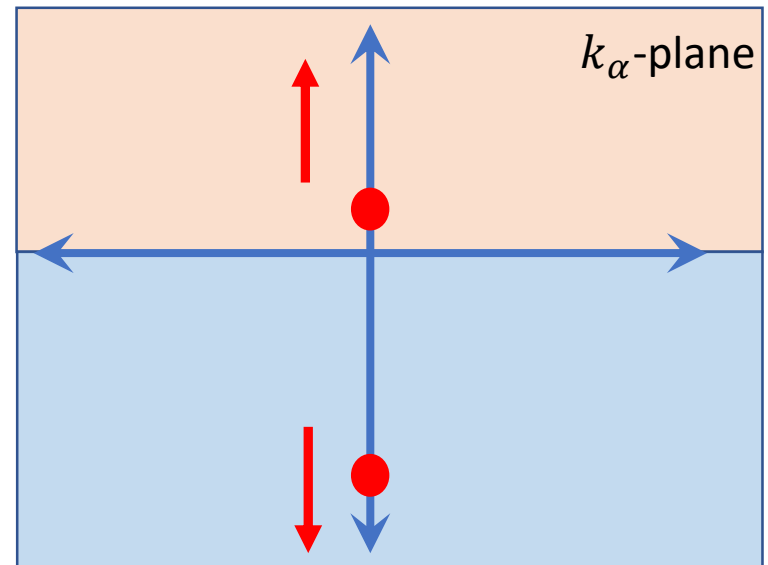
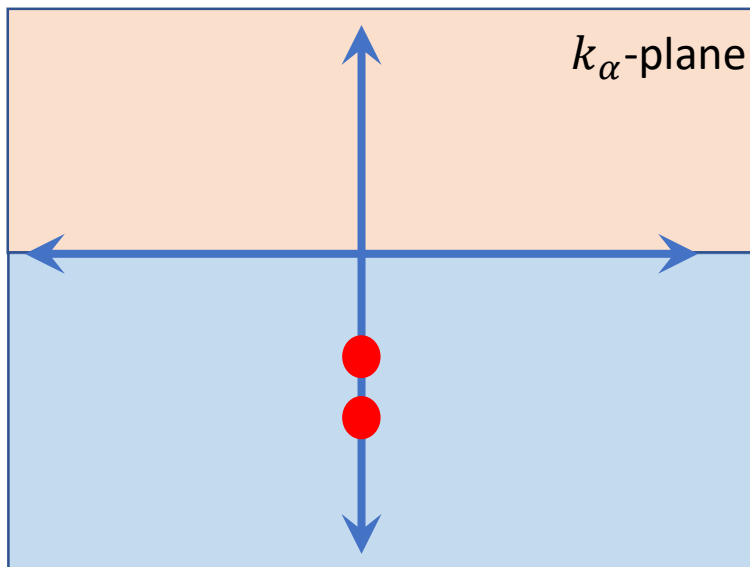
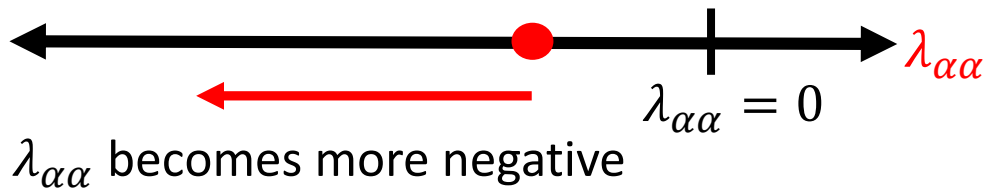
Poles in the single-channel case $\lambda_{12} = 0$

Pole-position condition:

$$\det[\tau(k_\alpha)^{-1}] = (\lambda^{-1})_{\alpha\alpha} - \frac{\pi\mu_\alpha\beta_\alpha^3}{2(k_\alpha + i\beta_\alpha)^2} = 0 \quad \Rightarrow \quad k_\alpha = -i\beta_\alpha \pm \sqrt{\frac{\pi\mu_\alpha\beta_\alpha^3\lambda_{\alpha\alpha}}{2}}$$

We can set $\lambda_{\alpha\alpha}$ to have either a bound state pole or a virtual state pole near the threshold.

$\beta_\alpha > 0$ is the cut-off parameter
 $\mu_\alpha > 0$ is the reduced mass
 $\lambda_{\alpha\alpha}$ is the potential parameter
 $\lambda_{\alpha\alpha} < 0$ attractive
 $\lambda_{\alpha\alpha} > 0$ repulsive



Poles in the single-channel case $\lambda_{12} = 0$

physical (complex energy) sheet: $k_1 = +\sqrt{2\mu_1 E}$

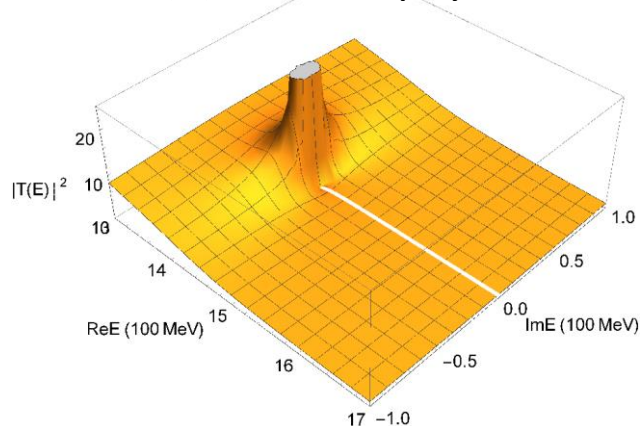
unphysical (complex energy) sheet: $k_1 = -\sqrt{2\mu_1 E}$

$$T(E) = -\pi\mu_1 k_1 \left[\frac{\beta_1^4}{(k_1^2 + \beta_1^2)^2} \right] \left[\frac{1}{\frac{1}{\lambda_1} - \frac{\pi\mu_1\beta_1^3}{2(k_1 + i\beta_1)^2}} \right]$$

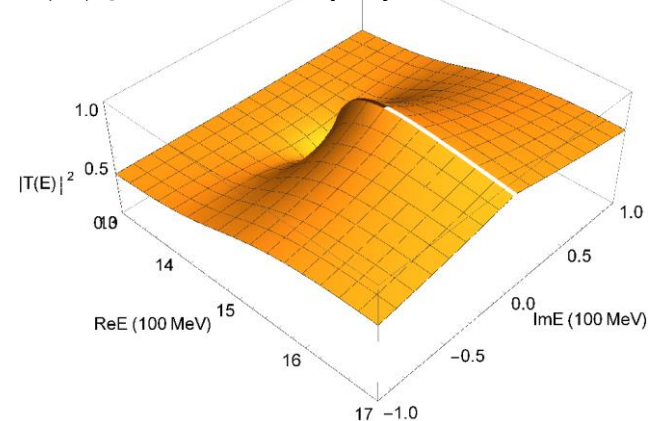
Parameters chosen give a bound state pole at $E = 1420 \text{ MeV}$.

$$\begin{aligned} \lambda_{11} &= -0.02371 \\ \beta_1 &= 1000 \text{ MeV} \\ \mu_1 &= 324 \text{ MeV} \\ \Theta_1 &= 1435 \text{ MeV} \end{aligned}$$

$|T(E)|^2$ in the physical sheet



$|T(E)|^2$ in the unphysical sheet



Poles in coupled-channel case

Details of pole-trajectory: $\det[\tau(E)^{-1}] = 0$

$$\left[(\lambda^{-1})_{11} - \frac{\pi\mu_1\beta_1^3}{2(k_1 + i\beta_1)^2} \right] \left[(\lambda^{-1})_{22} - \frac{\pi\mu_2\beta_2^3}{2(k_2 + i\beta_2)^2} \right] - (\lambda^{-1})_{12}(\lambda^{-1})_{21} = 0$$

- New set of unphysical sheets open
- Provide initial settings for channel 1 and channel 2 at $\lambda_{12} = 0$.
- Solve for k_1 and k_2 using:

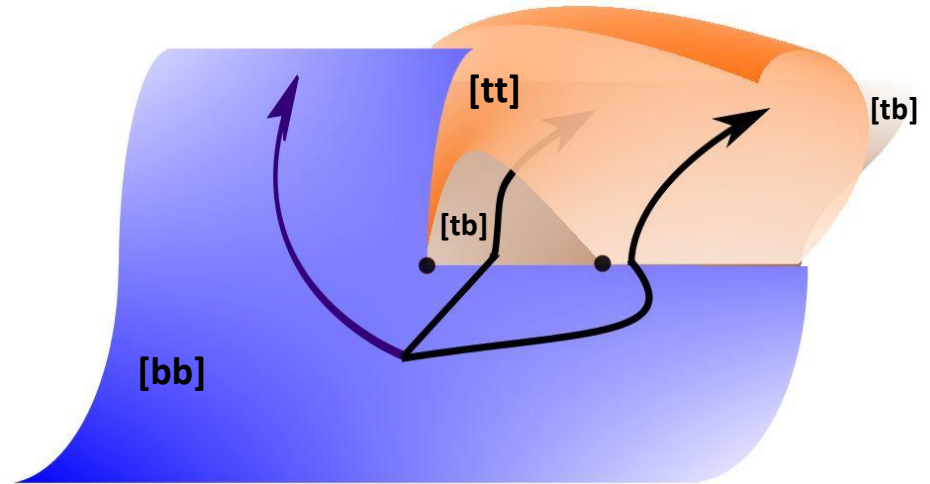
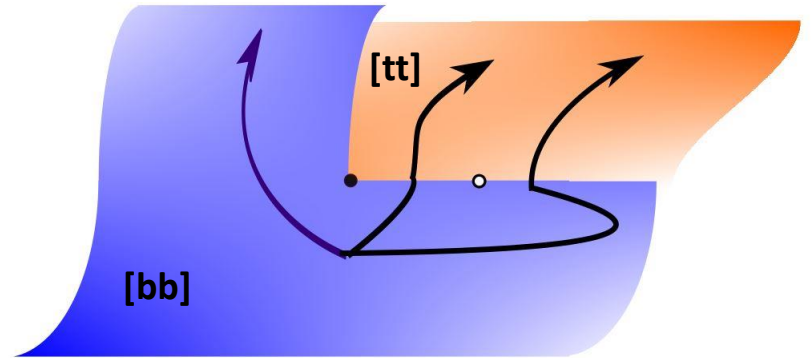
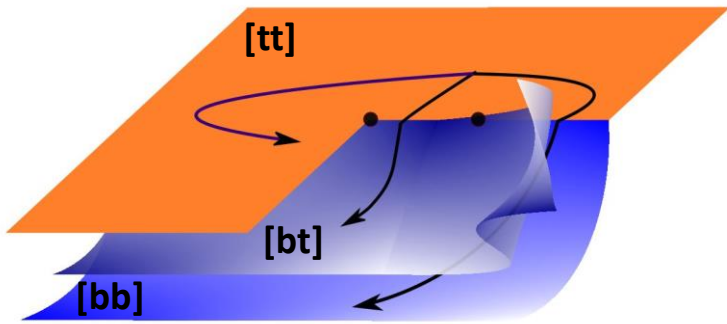
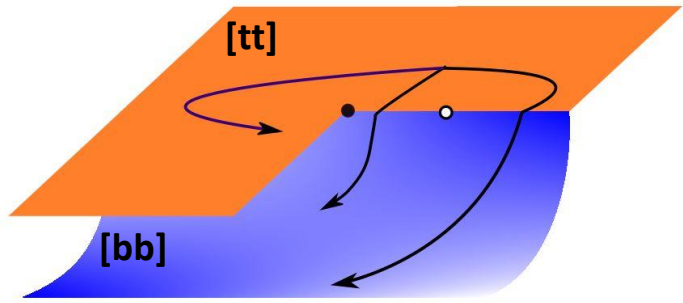
$$E = \frac{k_1^2}{2\mu_1} - \Theta_1 = \frac{k_2^2}{2\mu_2} - \Theta_2 \quad \text{and} \quad \det[\tau(k_1, k_2)^{-1}] = 0 \quad \Rightarrow \quad (k_1, k_2)$$

$$k_\alpha = \sqrt{2\mu_\alpha(E - \Theta_\alpha)}$$

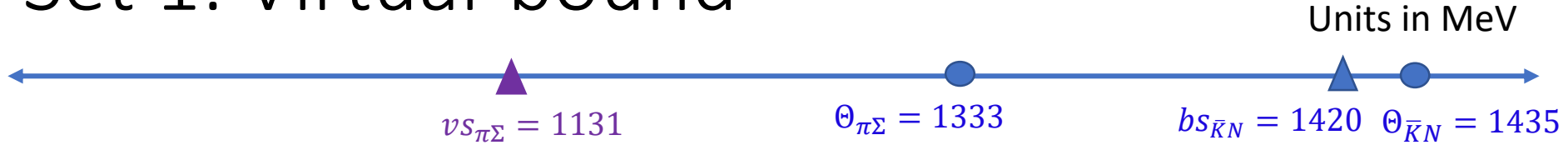
Riemann Sheet	Im k_1	Im k_2
[tt] (Physical sheet)	+	+
[bt] (Unphysical sheet)	-	+
[bb] (Unphysical sheet)	-	-
[tb] (Unphysical sheet)	+	-

Settings at $\lambda_{12} = 0$		
	Channel 1	Channel 2
Set 1	Virtual	Bound
Set 2	Virtual	Virtual
Set 3	Bound	Virtual
Set 4	Bound	Bound

Topology of the Riemann Sheets in a two-channel system

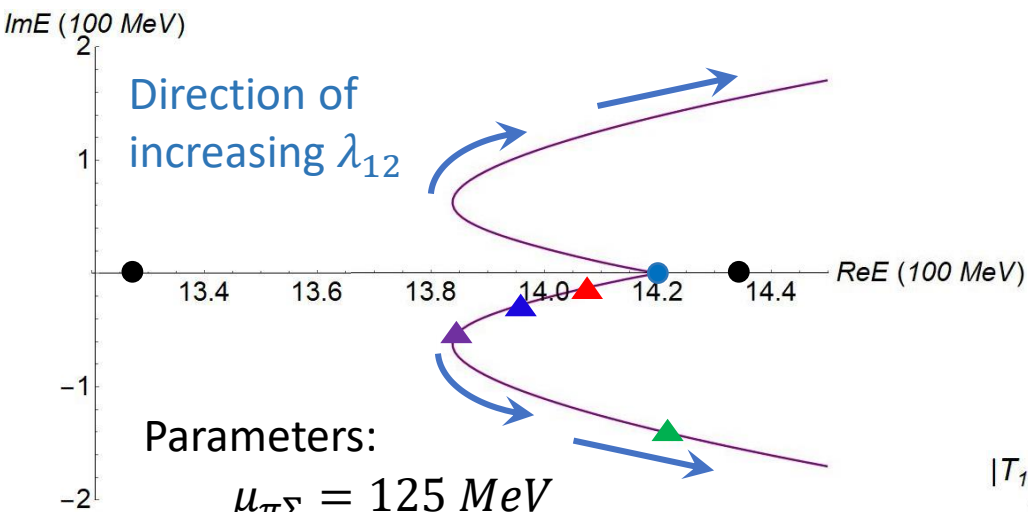


Set 1: Virtual-bound



Channel 1 Threshold at $\Theta_{\pi\Sigma} = 1333 \text{ MeV}$ with virtual state pole at $E = 1131 \text{ MeV}$

Channel 2 Threshold at $\Theta_{\bar{K}N} = 1435 \text{ MeV}$ with bound state poles at $E = 1420 \text{ MeV}$

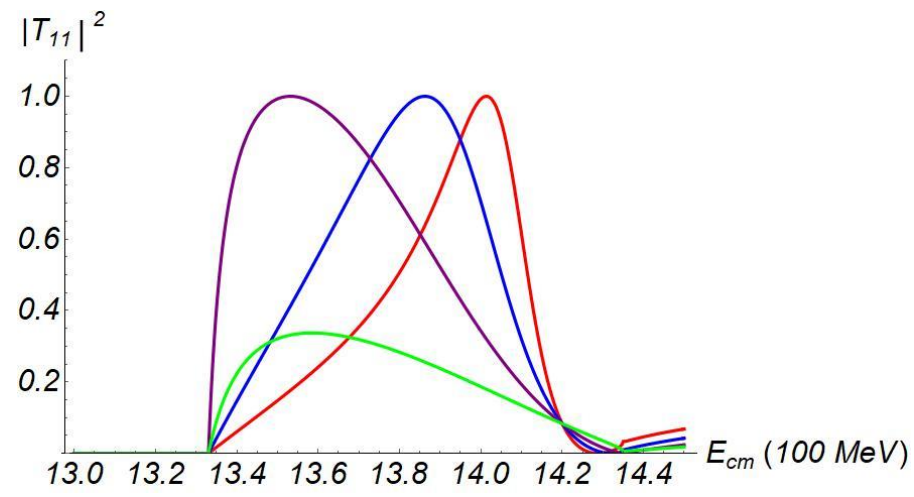


Parameters:

- $\mu_{\pi\Sigma} = 125 \text{ MeV}$
- $\lambda_{\pi\Sigma} = -0.03162$
- $\beta_{\pi\Sigma} = 1000 \text{ MeV}$
- $\mu_{\bar{K}N} = 324 \text{ MeV}$
- $\lambda_{\bar{K}N} = -0.02372$
- $\beta_{\bar{K}N} = 1000 \text{ MeV}$

λ_{12}	$Re(E_{pole})$	$Im(E_{pole})$
0.0069	1405.01	15.51
0.0087	1397.57	25.14
0.0110	1384.14	69.17
0.0142	1421.78	140.0

The pole moves in the unphysical [bt] sheet as λ_{12} is increased.

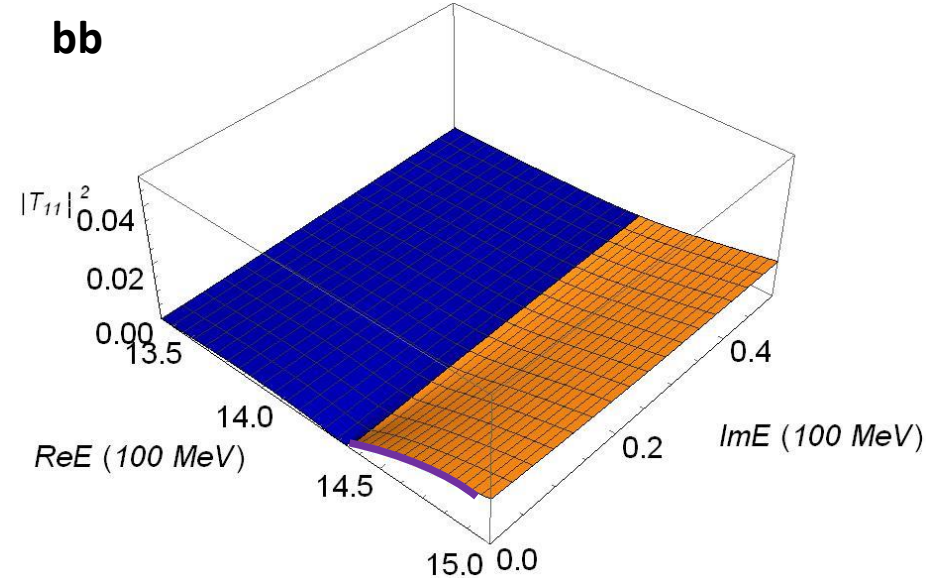
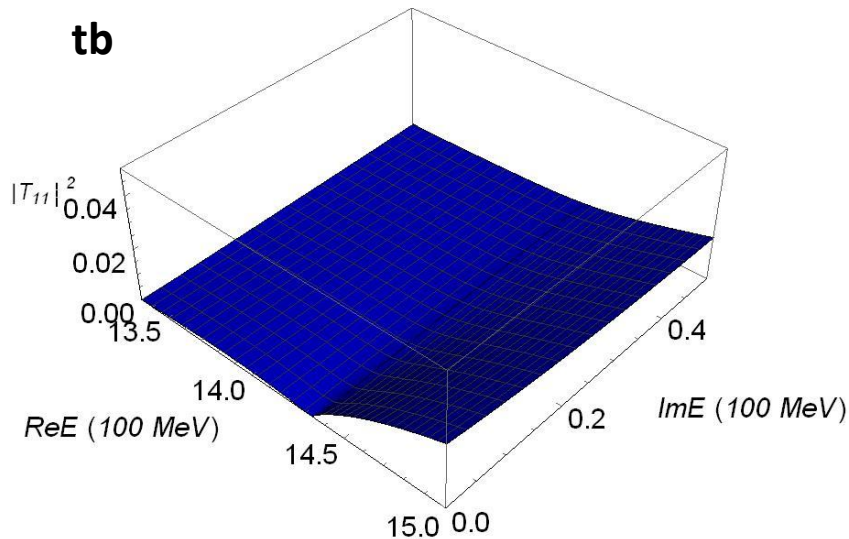
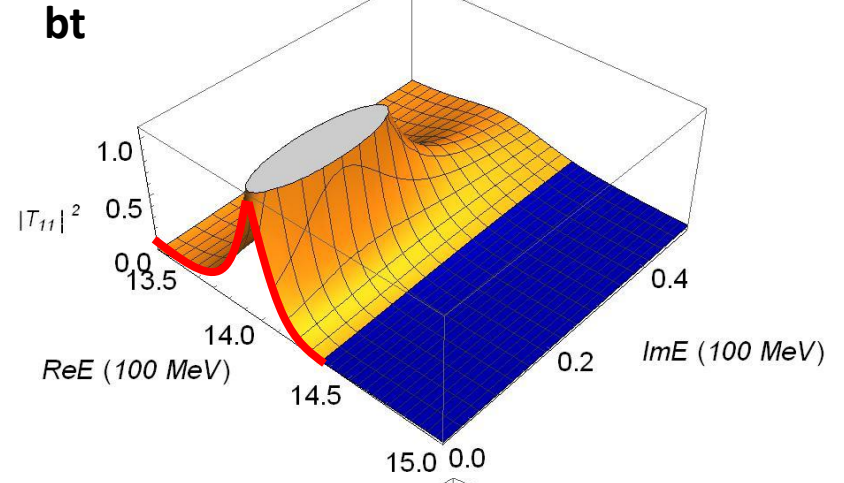
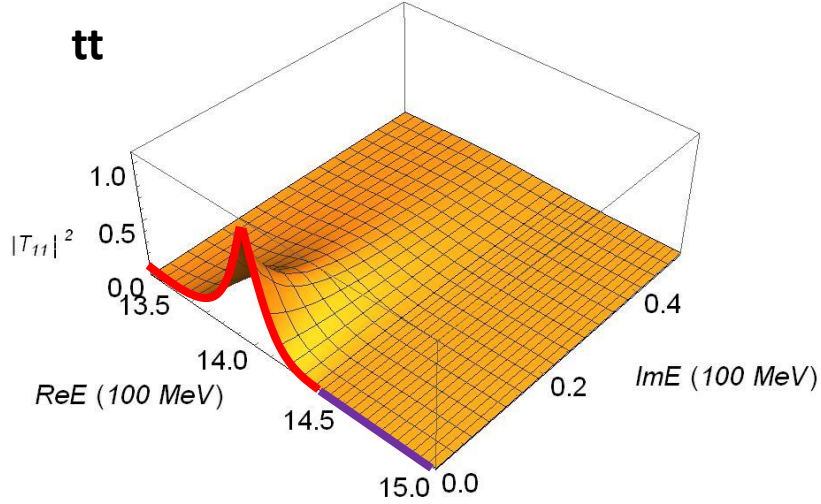
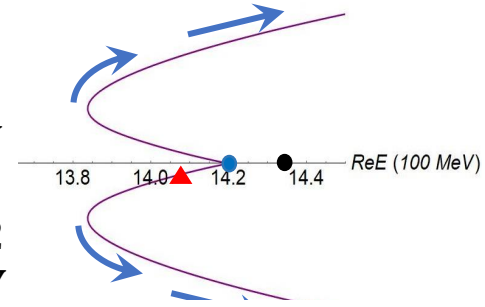


Set 1: Virtual-bound

λ_{12}	$Re(E_{pole})$	$Im(E_{pole})$
0.0069	1405.01	15.51

Parameters:

$$\begin{aligned} \mu_{\pi\Sigma} &= 125 \text{ MeV} \\ \lambda_{\pi\Sigma} &= -0.03162 \\ \beta_{\pi\Sigma} &= 1000 \text{ MeV} \\ \mu_{\bar{K}N} &= 324 \text{ MeV} \\ \lambda_{\bar{K}N} &= -0.02372 \\ \beta_{\bar{K}N} &= 1000 \text{ MeV} \end{aligned}$$



Set 2: Virtual-virtual

Units in 100 MeV

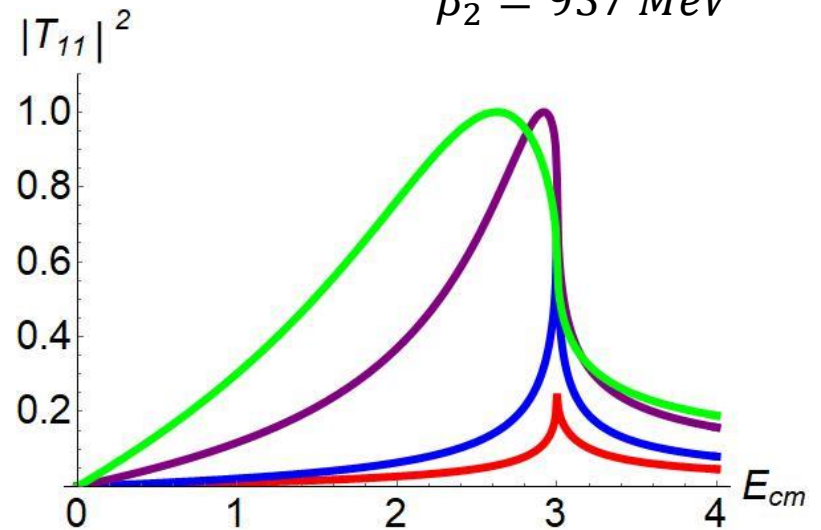
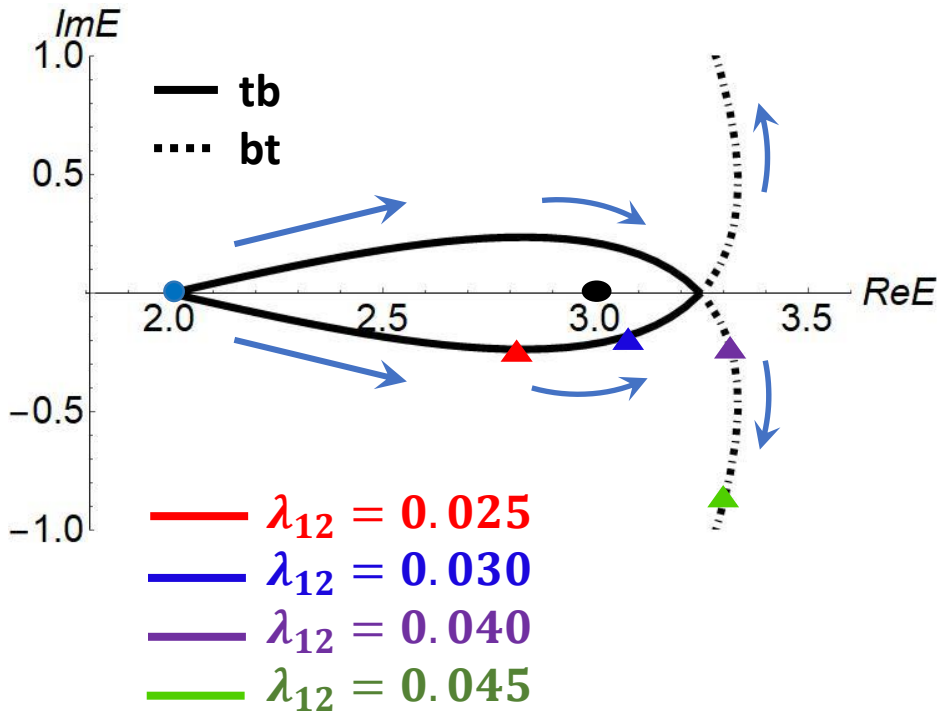


Channel 1 ($\Theta_1 = 0$): Virtual state poles at $E = -30$

Channel 2 ($\Theta_2 = 3$): Virtual state poles at $E = 2$

Parameters:

- $\mu_1 = 100 \text{ MeV}$
- $\lambda_1 = -0.00465$
- $\beta_1 = 1077 \text{ MeV}$
- $\mu_2 = 100 \text{ MeV}$
- $\lambda_2 = -0.04899$
- $\beta_2 = 937 \text{ MeV}$



In the solid line trajectory $Im(k_1) > 0$ and $Im(k_2) < 0$.
 In the dashed line trajectory $Im(k_1) < 0$ and $Im(k_2) > 0$.

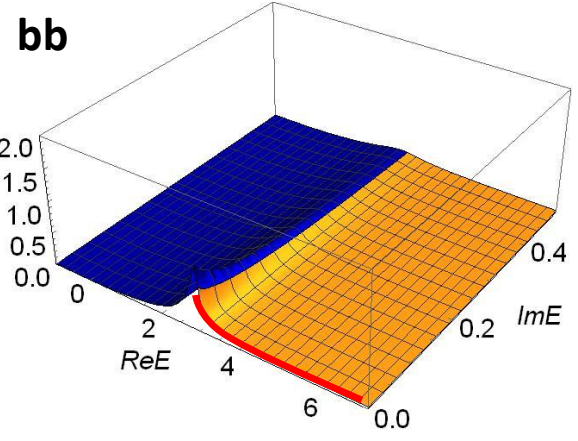
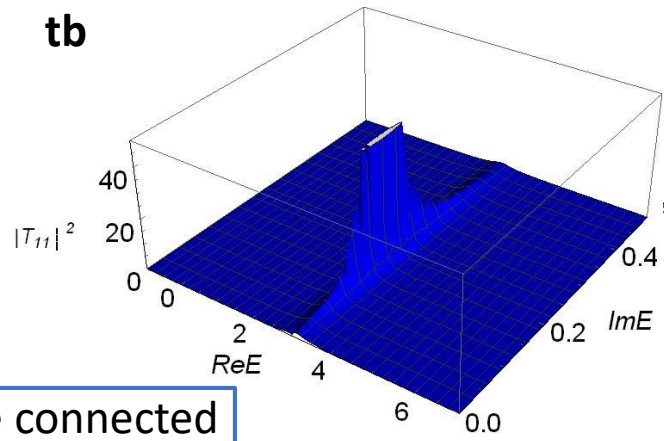
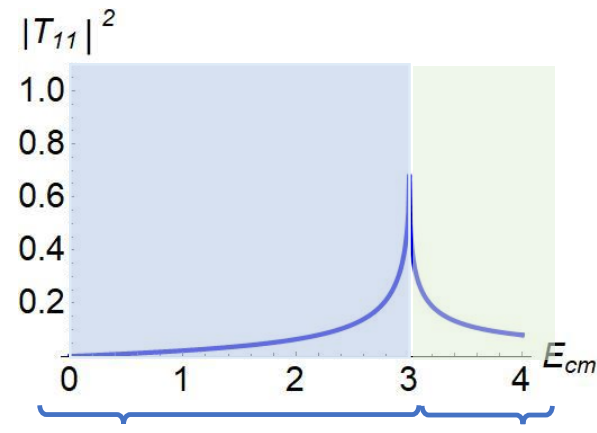
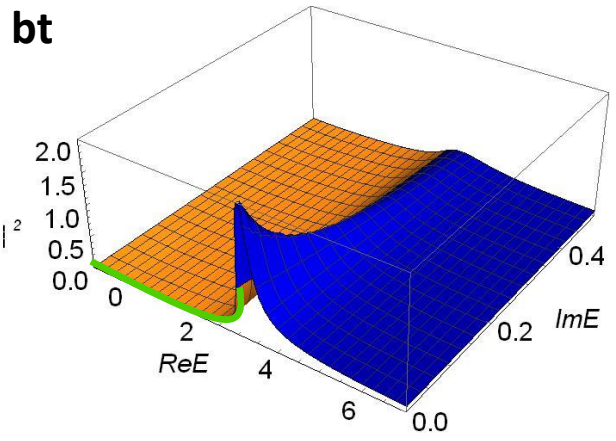
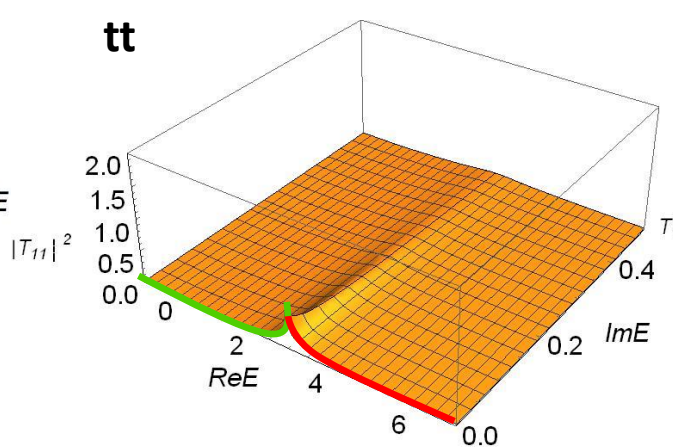
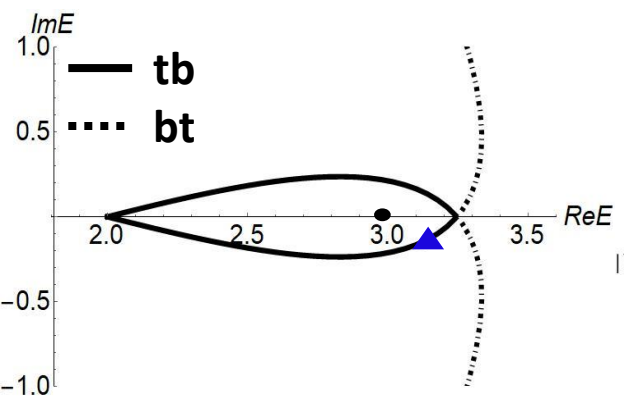
Set 2: Virtual-virtual

Units in 100 MeV



Channel 1 ($\Theta_1 = 0$): Virtual state poles at $E = -30$

Channel 2 ($\Theta_2 = 3$): Virtual state poles at $E = 2$



Structure connected to bt sheet

Structure connected to bb sheet

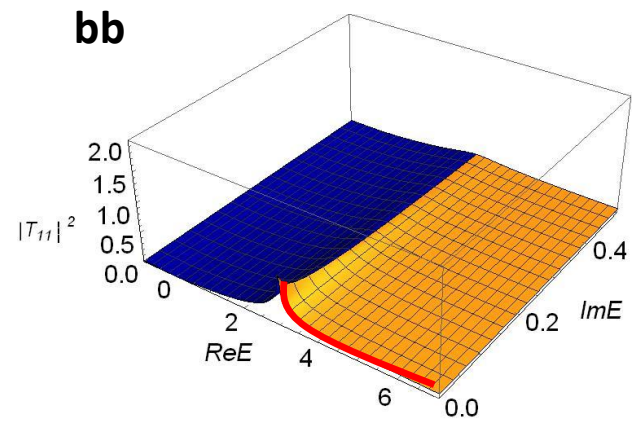
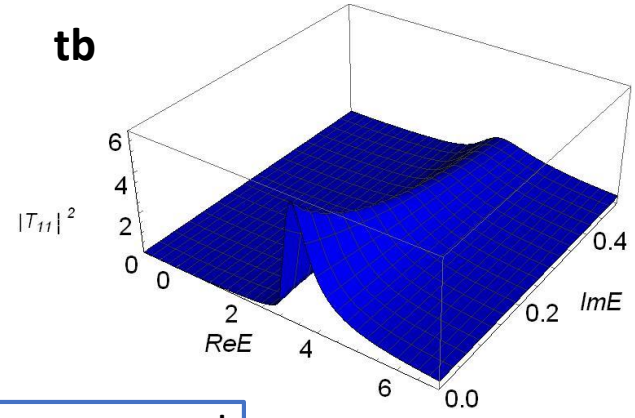
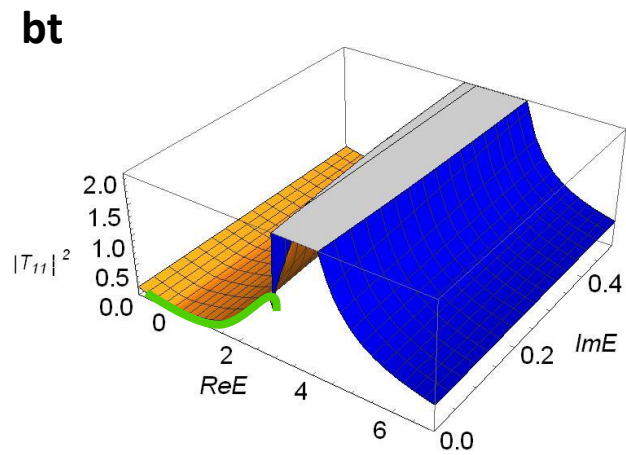
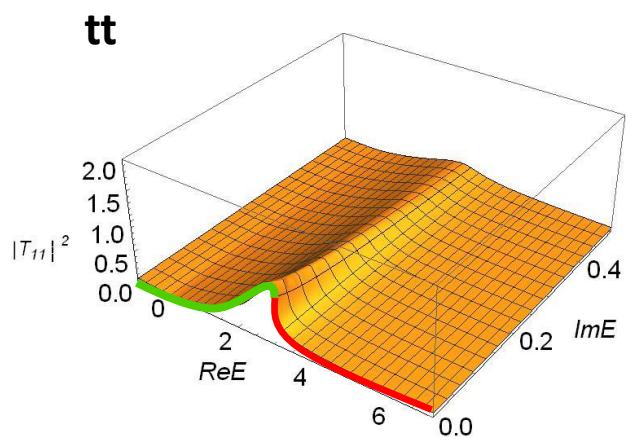
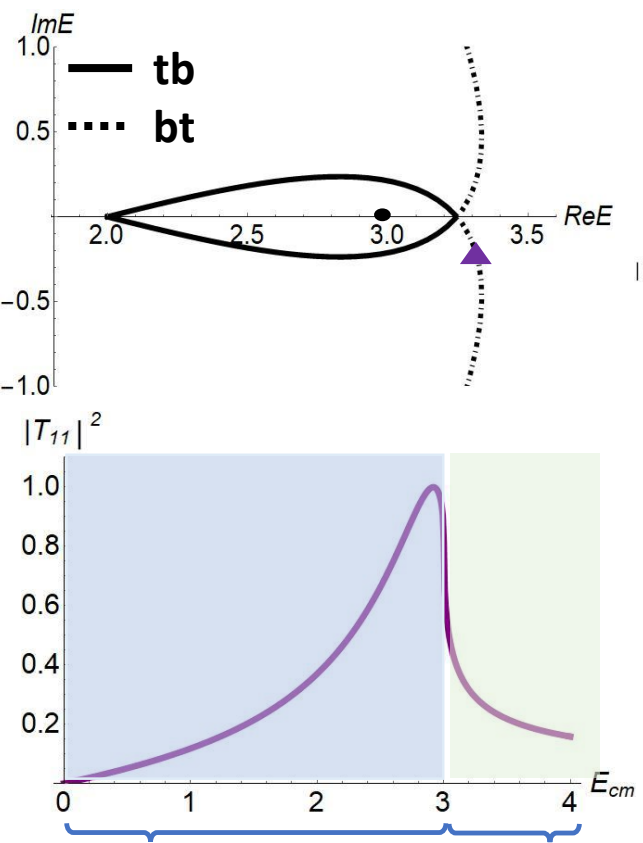
Set 2: Virtual-virtual

Units in 100 MeV



Channel 1 ($\theta_1 = 0$): Virtual state poles at $E = -30$

Channel 2 ($\theta_2 = 3$): Virtual state poles at $E = 2$



Structure connected to bt sheet

Structure connected to bb sheet

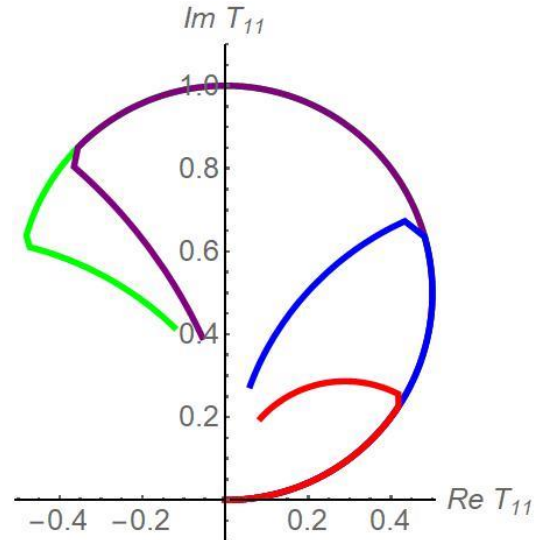
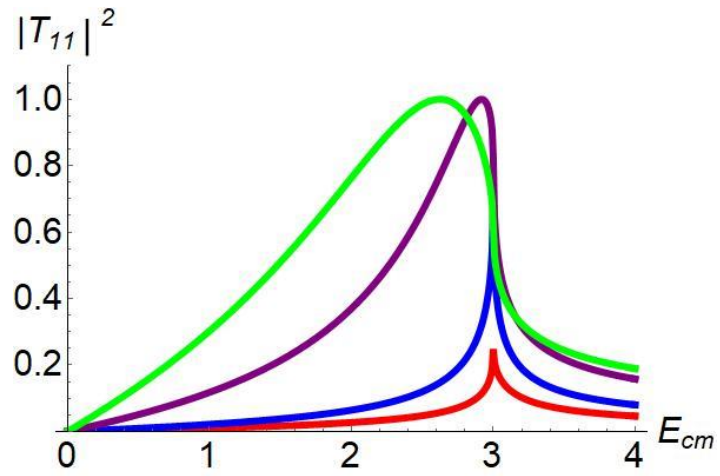
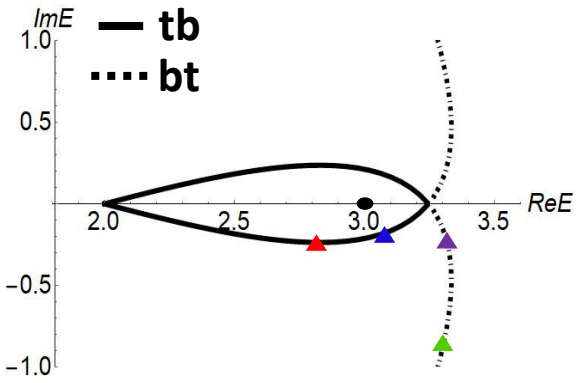
Set 2: Virtual-virtual

Units in 100 MeV



Channel 1 ($\Theta_1 = 0$): Virtual state poles at $E = -30$

Channel 2 ($\Theta_2 = 3$): Virtual state poles at $E = 2$



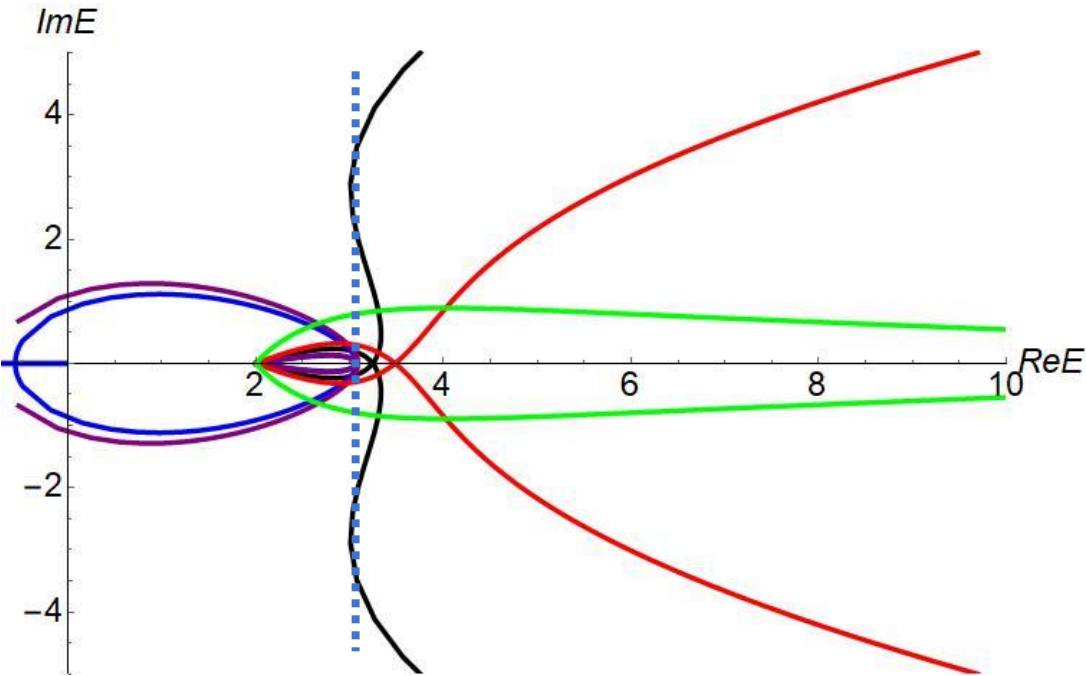
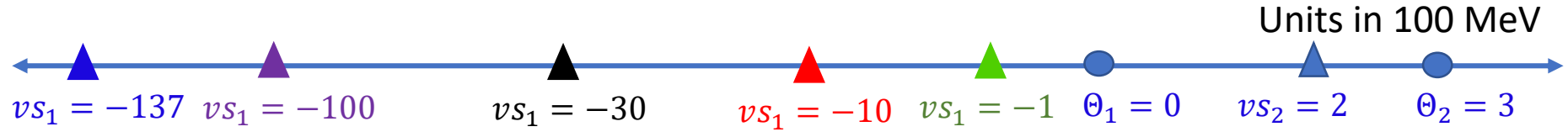
- $\lambda_{12} = 0.025$
- $\lambda_{12} = 0.030$
- $\lambda_{12} = 0.040$
- $\lambda_{12} = 0.045$

$E_{peak} = 2.918$
 $E_{peak} = 2.625$

$E_{\delta=\pi/2} = 2.918$
 $E_{\delta=\pi/2} = 2.625$

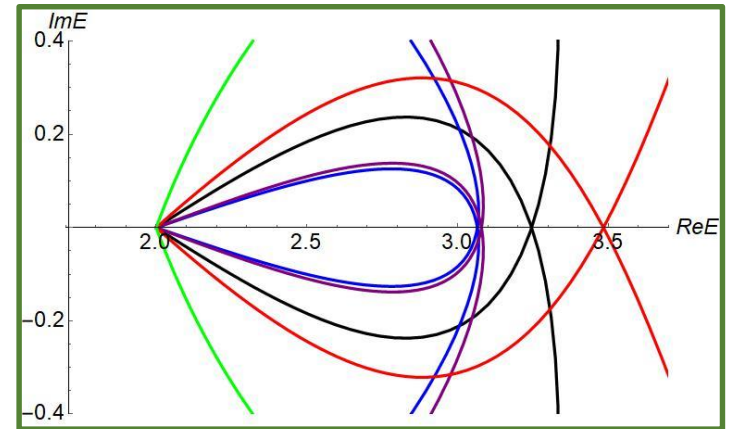
- The poles (**green** and **purple**) in the bt sheet are above the threshold (**black**).
- However, both the $|T_{11}|^2$ and the Argand diagram give resonance-like peak positions below the threshold.

Resonance and resonance-like structure



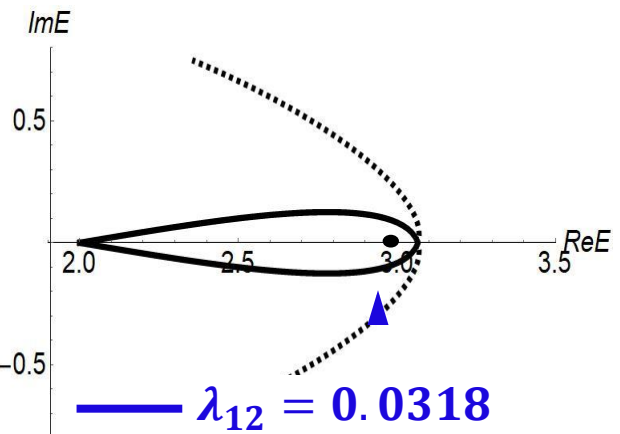
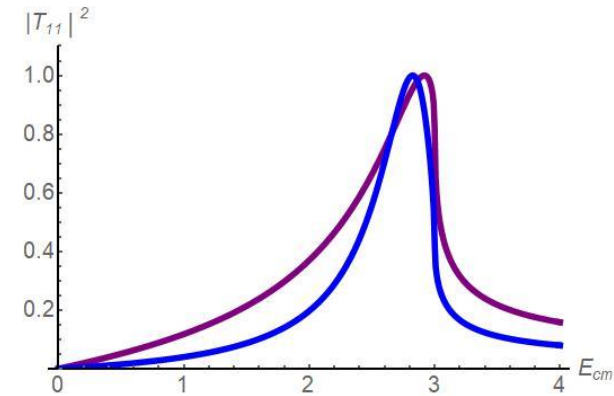
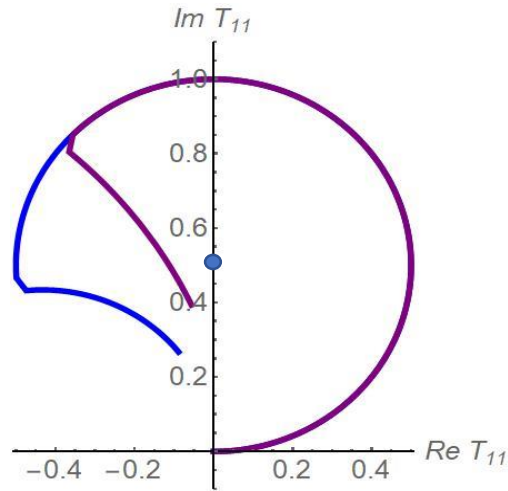
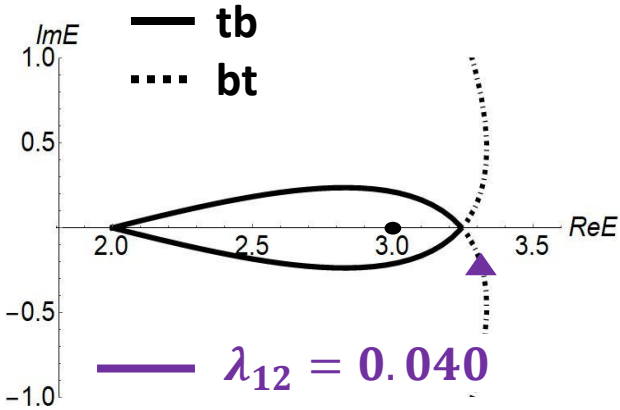
Position of pole in channel 1
when $\lambda_{12} = 0$.

$$k_1 = -i\beta_1 \pm \sqrt{\frac{\pi\mu_1\beta_1^3\lambda_{11}}{2}}$$



Choose two parametrization
with distinct trajectories

Resonance and resonance-like structure



The Argand diagram with $\delta(E = \Theta_2) > \frac{\pi}{2}$ is only an indication that a maximum $|T_{11}| = 1$ is reached but does not necessarily imply resonance.

The **purple case** is a resonance-like peak

- pole is no longer accessible in the physical region between the two thresholds.

The **blue case** is a resonance peak

- peak position coincides with the real part of the pole.

For a narrow peak-structure to be a resonance, the inelastic threshold should appear below the $T_{11} = i/2$.



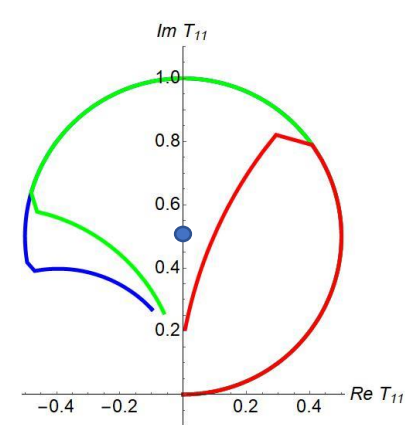
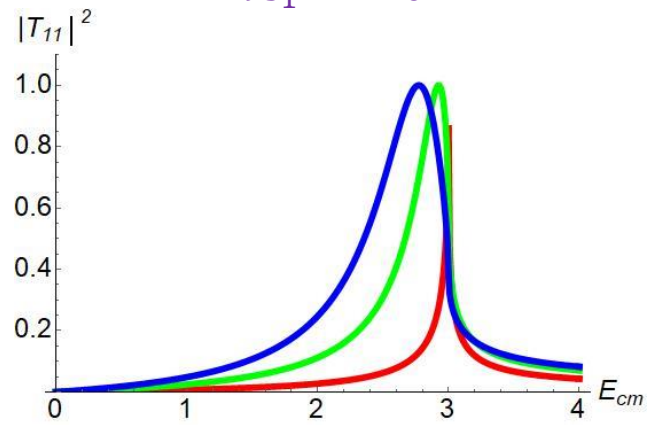
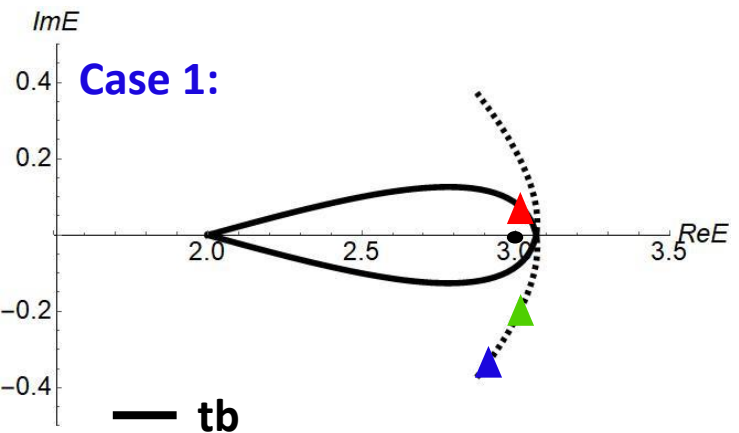
$$\delta(E = \Theta_2) > \frac{3\pi}{4}$$

Resonance and resonance-like structure

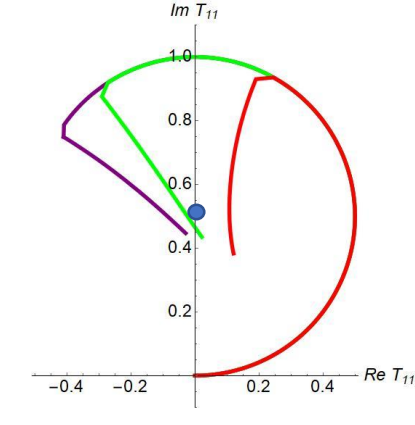
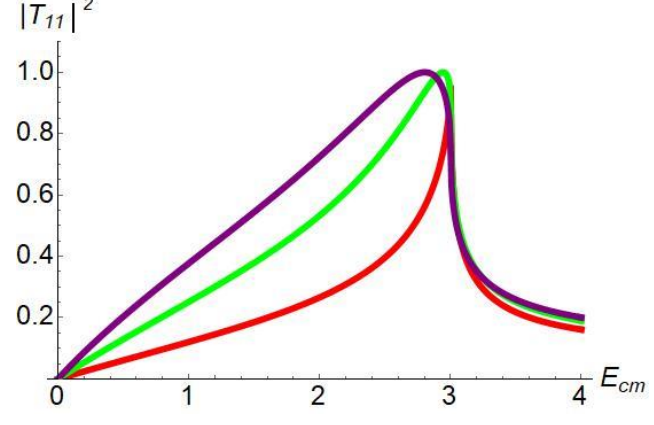
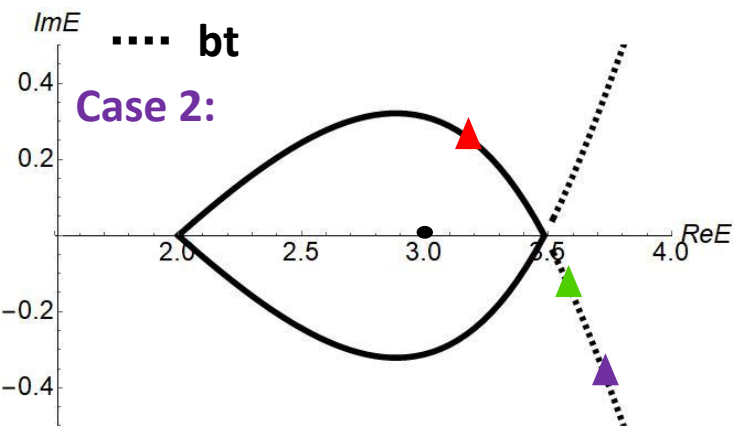
Units in 100 MeV



Case 1:



Case 2:



For a narrow peak-structure to be a resonance, the inelastic threshold should appear below the $T_{11} = i/2$.



$$\delta(E = \Theta_2) > \frac{3\pi}{4}$$

Summary

- Reviewed some fundamental properties of the S-matrix
- Introduced a separable potential model for coupled-channel system
 - Different parametrization in the zero-coupling limit results into different pole trajectories
 - Cusp structure in $|T_{11}|^2$ emerge if a pole in the inaccessible sheet crosses the threshold cut
 - Extraction of pole position based on the peak structure in the $|T_{11}|^2$ can be misleading.
 - The Argand diagram can be used to test if a peak structure is a resonance.